J. Cent. South Univ. (2016) 23: 708−720
DOI: 10.1007/s11771-016-3116-y

Springer

Safe retaining pressures for pressurized tunnel face using nonlinear failure criterion and reliability theory

YANG Xiao-li(杨小礼), YAO Cong(姚聪), ZHANG Jia-hua(张佳华)

School of Civil Engineering, Central South University, Changsha 410075, China

Abstract: Based on the active failure mechanism and passive failure mechanism for a pressurized tunnel face, the analytical solutions of the minimum collapse pressure and maximum blowout pressure that could maintain the stability of pressurized tunnel faces were deduced using limit analysis in conjunction with nonlinear failure criterion under the condition of pore water pressure. Due to the objective existence of the parameter randomness of soil, the statistical properties of random variables were determined by the maximum entropy principle, and the Monte Carlo method was employed to calculate the failure probability of a pressurized tunnel. The results show that the randomness of soil parameters exerts great influence on the stability of a pressurized tunnel, which indicates that the research should be done on the topic of determination of statistical distribution for geotechnical parameters and the level of variability. For the failure probability of a pressurized tunnel under multiple failure modes, the corresponding safe retaining pressures and optimal range of safe retaining pressures are calculated by introducing allowable failure probability and minimum allowable failure probability. The results can provide practical use in the pressurized tunnel engineering.

Key words: tunnel; limit analysis; nonlinear failure criterion; pore water pressure; retaining pressure

1 Introduction

With the rapid development of urban subway and significant improvement of shield machine technology, pressurized tunnels have become the mainstreams of urban tunnel engineering. However, due to the complexity of the strata where the pressurized tunnel passes through and the high density of buildings, the construction requirements are becoming strict. In the process of excavation, pressurized machine inevitably produces disturbance to the surrounding soils, and then induces a larger deformation, even a failure. When the retaining pressure is too small, the tunnel face easily collapses, while when the retaining pressure is too large, blowout damage would happen. Therefore, the determination of retaining pressure is the key to the stability of tunnel face, and the problem of retaining pressure is an important topic with great research value and practical significance.

Recently, the determination of retaining pressure for tunnel face has been studied. A cone failure mechanism was assumed for the tunnel face in order to obtain the minimum retaining pressure for tunnel face safety using limit analysis method, and the results agreed well with the results of centrifuge tests [1]. Multi-block failure mechanism was employed for tunnel, and the retaining pressures obtained were close to the results of centrifuge tests [2]. Considering that the assumption of velocity mutation occurring before a tunnel face is not reasonable, a velocity field was established. This changed from vertical gradually to horizontal direction to calculate the retaining pressure. HUANG et al [2] used the multi-block failure mechanism for a tunnel and obtained an analytical solution to retaining pressure with limit analysis method. According to the centrifuge test results, SUBRIN and WONG [3] built a new 3D failure mechanism for a pressurized tunnel, and obtained different ranges of earth pressure based on limit analysis method. With reference to the numerical simulation results, KLAR et al [4] established 2D and 3D failure mechanism for tunnel face, and computed the failure probability under different retaining pressures using limit analysis and probabilistic methods.

In practical engineering, a large number of experiments show that the soil obeys nonlinear failure criterion at failure and linear criterion is just a special case [5−6]. Both an active failure mechanism and a passive failure mechanism are established in this work. With a consideration of the influence of pore water, the retaining pressure for a pressurized tunnel is obtained using limit analysis theory with the tangent method for

Foundation item: Project(2013CB036004) supported by the National Basic Research Program of China; Project(51378510) supported by the National Natural Science Foundation of China
Received date: 2015−01−12; **Accepted date:** 2015−05−07
Corresponding author: YANG Xiao-li, Professor, PhD; Tel: +86−14789933669; E-mail: yangky@aliyun.com

nonlinear analysis. And on account of the objective existence of the parameter randomness of soil and its great impact on stability of geotechnical structures, reliability theory is applied to study the range of safe retaining pressures. The results can provide important guidance for the design and construction of pressurized tunnels.

2 Definitions and theorems

2.1 Nonlinear failure criterion and tangent method

In geotechnical engineering, materials are generally assumed to follow linear Mohr-Coulomb (MC) failure criterion. However, in fact, most geotechnical materials obey nonlinear failure criterion, namely the relationship between shear stress and normal stress is not linear, and the expression is written as follows:

$$\tau = c_0(1+\sigma_n/\sigma_t)^{1/m} \tag{1}$$

where τ is shear stress; σ_n is normal stress; c_0 is initial cohesion; σ_t is axial tensile stress; m is nonlinear coefficient. It can be found that when m=1, the relationship between shear stress and normal stress is degenerated to be linear. Therefore, linear MC failure criterion is just a special case of nonlinear failure criterion.

For MC materials, the analysis and calculation of shear strength usually refer to two important mechanics index, namely the cohesion c and internal friction angle φ. However, if geotechnical materials obey the nonlinear failure criterion, the expression of Eq. (1) does not contain the parameters c and φ. So, it is difficult to introduce nonlinear failure criterion to the analysis of the shear strength of geotechnical materials, which is the reason why nonlinear failure criterion is seldom used in geotechnical engineering.

In order to solve this problem, the generalized tangent method is employed, as shown in Fig. 1. In stress coordinate system, nonlinear failure criterion is characterized by a curved line, drawing a tangential line to the curve at the location of tangency point M which presents an angle of φ_t to the direction of σ_n-axis, and the intercept of the straight line c_t with respect to the τ-axis. In this case, φ_t and c_t are the corresponding internal frictional angle and cohesion of point M under nonlinear failure criterion. Consequently, this tangent method can be utilized to obtain above two parameters of geomaterials which follow nonlinear failure criterion. Therein, the expression of the tangential line is

$$\tau = c_t + \sigma_n \tan\varphi_t \tag{2}$$

With Eq. (1) and Eq. (2), Eq. (3) can be easily obtained. The nonlinear failure criterion will be introduced by Eq. (3) in the analysis and calculation of

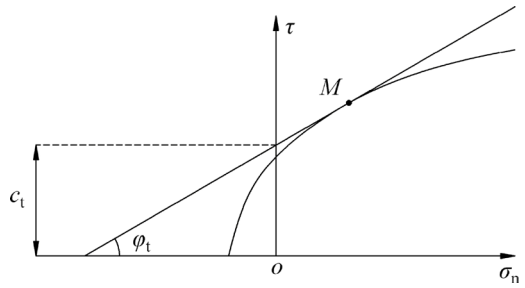

Fig. 1 Tangential line of nonlinear Mohr-Coulomb failure criterion

the shear strength in this work. It is noticed that, unlike linear MC failure criterion, the cohesion c_t and internal friction angle φ_t of nonlinear failure criterion are variables:

$$c_t = \frac{m-1}{m}c_0\left(\frac{m\sigma_t\tan\varphi_t}{c_0}\right)^{\frac{1}{1-m}} + \sigma_t\tan\varphi_t \tag{3}$$

2.2 Upper bound theorem with effect of pore water pressure

The pore water pressure has vital impact on the material shear strength and the stability of geotechnical structures. In engineering, pore water pressure is generally researched by the two methods [7−8]. The pore water pressure can be determined based on the positions of flow net of ground water and the saturation line, and it can be regarded as a component of soil gravity, and is also employed in this work. The expression can be written as follows:

$$u = r_u\gamma z \tag{4}$$

where u is pore water pressure; r_u is the coefficient of pore water pressure; γ is soil weight per volume; z represents the vertical distance between the soil and the ground surface.

The pore water pressure is considered as the internal force or the external force when being introduced into upper bound theorem [9−10]. The previously published works have shown that the two methods lead to the same results, which can be proven by the following equation:

$$-\int_V u\dot{\varepsilon}_{ij}\mathrm{d}V - \int_S u\boldsymbol{n}_i\boldsymbol{v}_i\mathrm{d}S = -\gamma_w\int_V\frac{\partial h}{\partial x_i}\boldsymbol{v}_i\mathrm{d}V + \gamma_w\int_V\frac{\partial Z}{\partial x_i}\boldsymbol{v}_i\mathrm{d}V \tag{5}$$

where u is the pore water pressure; $\dot{\varepsilon}_{ij}$ is the volumetric strain rate; V is the volume; $\boldsymbol{n}_i$ is the outward unit normal vector of failure surface; $\boldsymbol{v}_i$ is the velocity of the failure mechanism; S is the failure surface; γ_w is the unit weight of water; h is the water head; Z is the elevation head. The first integral on the left-hand side is the power of pore-water pressure on soil volumetric strain and the

second one on the left is the work rate of pore-water pressure acting on the boundary. The first term on the right-hand side is the power of seepage force, and the last is the work rate of buoyancy force.

In this work, pore water pressure is taken as the external force to be introduced into upper bound theorem. The upper bound theorem of limit analysis could be expressed as: under any kinematically admissible velocity field, the active load calculated through equating the external work rate to the internal energy dissipation of rock/soil masses is not less than the real ultimate load [11−12]. To sum up, the upper bound theorem under the effect of pore water pressure is expressed as

$$\int_V \sigma_{ij}\dot{\varepsilon}_{ij}\mathrm{d}V \geq \int_S \boldsymbol{T}_i\boldsymbol{v}_i\mathrm{d}S + \int_V \boldsymbol{F}_i\boldsymbol{v}_i\mathrm{d}V - \int_V u_i\dot{\varepsilon}_{ij}\mathrm{d}V - \int_S u_i\boldsymbol{n}_i\boldsymbol{v}_i\mathrm{d}S \tag{6}$$

where the first integral represents the internal energy dissipation; the second one is the dot product of external load $\boldsymbol{T}_i$ and the velocity vector $\boldsymbol{v}_i$ along the boundary S, and the third one is the dot product of volume force $\boldsymbol{F}_i$ and the velocity vector $\boldsymbol{v}_i$ within the region V; the fourth one is the power of pore-water pressure over the region V; the last is the work rate of pore-water pressure acting on the boundary S.

2.3 Probability density function based on maximum entropy principle

Entropy of a random variable shows the uncertainty degree of the random variable in the whole domain. For a continuous random variable X, the entropy is defined as

$$H = -\int_R f(x)\ln f(x)\mathrm{d}x \tag{7}$$

where H is the entropy of random variable X, $f(x)$ is the probability density function of random variable X, and R is the domain of random variable X.

The maximum entropy principle can be described as: the uncertainty of the random variable is the largest when entropy is the largest, which also means that the random variable has a 'minimum bias'. Therefore, the probability distribution based on the principle of maximum entropy principle is the most close to the real probability distribution. The probability density function based on maximum entropy principle is also called optimal probability density function. The probability distribution model of random variable X on the basis of the maximum entropy principle can be expressed as

$$\text{Max.}\quad H = -\int_R f(x)\ln f(x)\mathrm{d}x \tag{8}$$

$$\text{s.t.}\begin{cases}\int_R f(x)\mathrm{d}x = 1\\ \int_R x^i f(x)\mathrm{d}x = \mu_i\ \ (i = 0,1,2,\cdots,n)\end{cases} \tag{9}$$

where Eq. (8) is the maximum of objective function H, Eq. (9) is the constraint of objective function H, μ_i is the i order origin moment of random variable X, and n is the order of moment.

In order to obtain the maximum of objective function H, Lagrange function can be established using Lagrange multiplier method and it can be expressed as

$$L = H + \lambda_0\left(\int_R f(x)\mathrm{d}x - 1\right) + \sum_{i=1}^{n}\lambda_i\left(\int_R x^i f(x)\mathrm{d}x - \mu_i\right) \tag{10}$$

where λ_i is Lagrange multiplier. According to Fermat's Theorem, maximization of Eq. (10) requires

$$\frac{\partial L}{\partial f(x)} = 0 \tag{11}$$

Then, the analytical solution of the maximum entropy can be obtained:

$$f(x) = \exp\left(-\sum_{i=0}^{n}\lambda_i x^i\right) \tag{12}$$

By substituting Eq. (12) into Eq. (9), the following equation is obtained

$$F(\lambda_0,\lambda_1,\cdots,\lambda_n) = \int_R x^i \exp\left(-\sum_{i=0}^{n}\lambda_i x^i\right)\mathrm{d}x - \mu_i = 0 \quad (i = 0,\ 1,\ 2,\ \cdots,\ n) \tag{13}$$

Equation (13) is a system of nonlinear equations, which contains n+1 unknowns. Then, λ_i can be obtained using Newton's iteration method, and the probability density function $f(x)$ based on maximum entropy principle can be acquired by substituting λ_i into Eq. (12).

The existing research results [13−17] show that: (1) Probability distribution based on the principle of maximum entropy is a normal distribution, when the mean and variance of the continuous random variable X are constants; (2) Probability distribution based on the principle of maximum entropy is lognormal, when the geometric mean and standard deviation of logarithm for the continuous random variable X are constants. Therefore, in this work, it is assumed that the probability distribution of geotechnical materials' parameters follows normal distribution or lognormal distribution.

2.4 Basic principle of Monte Carlo method

Monte Carlo method is also called as stochastic simulation method, random-sampling technique or statistical experiment method. It offers an approach which can estimate the failure probability of structure through the structure failure frequency. At present, the Monte Carlo method is considered to be a relatively accurate method in structural reliability analysis.

According to the law of large numbers, it is assumed that x_1, x_2, ⋯, x_n are n independent random

variables, which come from the same matrix and share the same distribution, namely, with the same mathematical expectation μ and variance σ^2. Then, as for $\varepsilon>0$, we have

$$\lim_{n\to\infty} P\left\{\left|\frac{1}{n}\sum_{i=1}^{n} x_i - \mu\right| \geq \varepsilon\right\} = 0 \tag{14}$$

The probability of random event A is denoted as $P(A)$. And in n independent tests, event A occurs m times, then the frequency is $W(A)=m/n$. Then, for any $\varepsilon>0$, we can get

$$\lim_{n\to\infty} P\left\{\left|\frac{m}{n} - P(A)\right| < \varepsilon\right\} = 1 \tag{15}$$

Reliability calculation of structures (or probability of failure) by Monte Carlo method comprises the following steps: (1) All random variables are sampled with many times, which have influence on the structure; (2) The sampling values of random variables are substituted one by one into all structural performance functions to determine whether the structure is safe or not; (3) All the number of safe structures (or failure) is recorded; (4) The reliability or failure probability of the structure is calculated.

According to Eq. (15), when the sampling number n is large enough, the result is close to the exact value, and then the statistical function can be written as follows:

$$P_{\mathrm{f}} = \frac{1}{n}\sum_{i=1}^{n} I(X) = \frac{1}{n}\sum_{i=1}^{n} I(X_1,\ X_2,\ \cdots,\ X_n) \tag{16}$$

where the performance function is denoted as

$$I(X) = I(X_1, X_2, \cdots, X_n) = \begin{cases} 1, \text{ if } G(X_1, X_2, \cdots, X_n) < 0 \\ 0, \text{ if } G(X_1, X_2, \cdots, X_n) \geq 0 \end{cases} \tag{17}$$

By substituting n random numbers successively into Eq. (17), the sum n_{f} of the number of failure can be obtained, and the reliability can be expressed as

$$R_{\mathrm{s}} = 1 - P_{\mathrm{f}} = 1 - \frac{n_{\mathrm{f}}}{n} \tag{18}$$

And the corresponding failure probability can be written as

$$P_{\mathrm{f}} = \frac{n_{\mathrm{f}}}{n} \tag{19}$$

The structural reliability can also be derived through the number of safe structures, that is,

$$R_{\mathrm{s}} = \frac{1}{n}\sum_{i=1}^{n} I'(X) = \frac{1}{n}\sum_{i=1}^{n} I'(X_1, X_2, \cdots, X_n) \tag{20}$$

where the performance function is denoted as

$$I'(X) = I'(X_1, X_2, \cdots, X_n) = \begin{cases} 1, \text{ if } G(X_1, X_2, \cdots, X_n) > 0 \\ 0, \text{ if } G(X_1, X_2, \cdots, X_n) \leq 0 \end{cases} \tag{21}$$

By substituting n random numbers successively into Eq. (21), the sum n_{s} of the number of safety can be obtained, and the reliability can be expressed as

$$R_{\mathrm{s}} = \frac{n_{\mathrm{s}}}{n} \tag{22}$$

Consequently, the corresponding failure probability is

$$P_{\mathrm{f}} = 1 - R_{\mathrm{s}} = 1 - \frac{n_{\mathrm{s}}}{n} \tag{23}$$

3 Failure mechanisms and velocity field

In accordance with the requirements of the limit analysis, a failure mechanism of excavation face should be established before solving the retaining pressure of the pressurized tunnel, and the failure mechanism is usually constructed with reference to engineering practice, model tests and numerical simulation. As to the pressurized tunnel, LECA and DORMIEUX [1] proposed two failure mechanisms based on the results of centrifuge tests: (1) the first failure mechanism is composed of a rigid block, and the entire rigid block slides at failure, (2) the second one contains two rigid blocks, and the lower block is moving towards the excavation face pushed by the upper one. Subsequently, KLAR et al [4] established 2D and 3D failure mechanism for tunnel face, which makes the failure mechanism more reasonable.

On the basis of the above research results and the characteristics of the pressurized tunnel, two failure mechanisms are established, as shown in Fig. 2. AB is the face of the pressurized tunnel, D represents the diameter of tunnel, and C refers to cover depth. While the pressurized tunnel is under excavation, it may present two kinds of failure styles under the action of pore water pressure u: (1) when the retaining pressure is small, the soil in front of the face tends to collapse, namely active failure mechanism, as shown in Fig. 2(a), and the vertex O may be under or above the ground surface, and (2) when the retaining pressure is too large, the soil in front of the face may be squeezed out, namely passive failure mechanism, as shown in Fig. 2(b).

In addition, according to the characteristics of the active failure mechanism and passive failure mechanism, the corresponding velocity fields are built respectively, as shown in Fig. 3. The velocity field of active failure mechanism is illustrated in Fig. 3(a). From right to left, the apex angles are $\beta+2\varphi_{\mathrm{t}}$, α_1, α_2, ⋯, α_{n-1} in the order; the obtuse angles are $\pi-\beta$, $\pi/2-\alpha_1+2\varphi_{\mathrm{t}}$, $\pi/2-\alpha_2+$

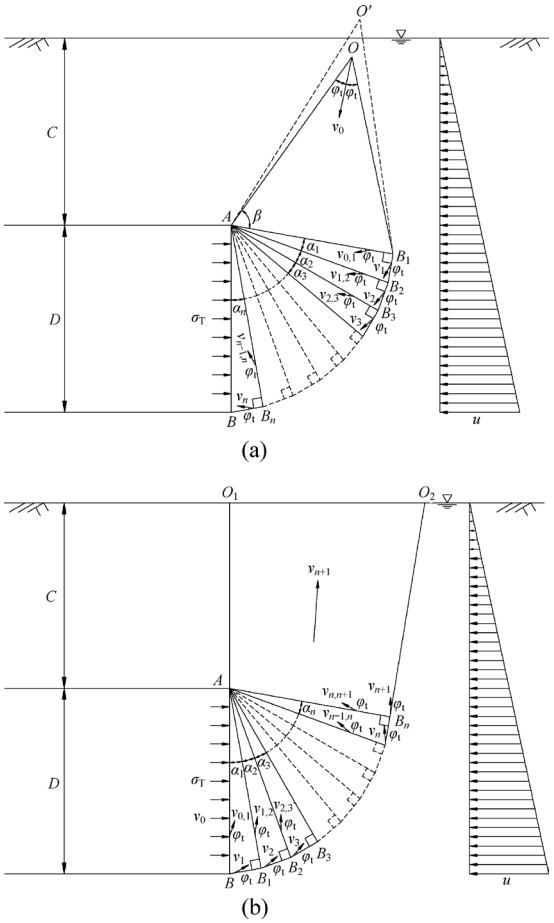

Fig. 2 Failure mechanisms of pressurized tunnel: (a) Active failure mechanism; (b) Passive failure mechanism

$2\varphi_t$, ⋯, $\pi/2-\alpha_{n-1}+2\varphi_t$ and the acute angle is $\pi/2-2\varphi_t$. The velocity field of passive failure mechanism is illustrated in Fig. 3(b). From the bottom to the up, the apex angles are $\alpha_1+\varphi_t$, α_2, α_3, ⋯, α_n, $\pi/2-\sum_{i=1}^{n}\alpha_i-2\varphi_t$ in order; the first obtuse angle is $\pi/2+\varphi_t$, other obtuse angles are $\pi/2+2\varphi_t$, and the acute angles are $\pi/2-\alpha_1-2\varphi_t$, $\pi/2-\alpha_2-2\varphi_t$, $\pi/2-\alpha_3-2\varphi_t$, $\pi/2-\alpha_n-2\varphi_t$, $\sum_{i=1}^{n}\alpha_i$.

Then, according to Fig. 3(a), the velocities of active failure mechanism can be derived:

$$v_1=\frac{\sin(\alpha-\beta)}{\sin(\pi/2-\alpha-\varphi_t)}v_0 \tag{24}$$

$$v_{0,1}=\frac{\sin(\pi/2+2\varphi_t-\alpha-\beta)}{\sin(\pi/2-\alpha-\varphi_t)}v_0 \tag{25}$$

$$v_i=\frac{\sin(\pi/2-\alpha_{i-1}+\varphi_t)}{\sin(\pi/2-\alpha-\varphi_t)}v_{i-1}\ (i=2,\cdots,n) \tag{26}$$

$$v_{i-1,i}=\frac{\sin\alpha_{i-1}}{\sin(\pi/2-\alpha-\varphi_t)}v_{i-1}\ (i=2,\cdots,n) \tag{27}$$

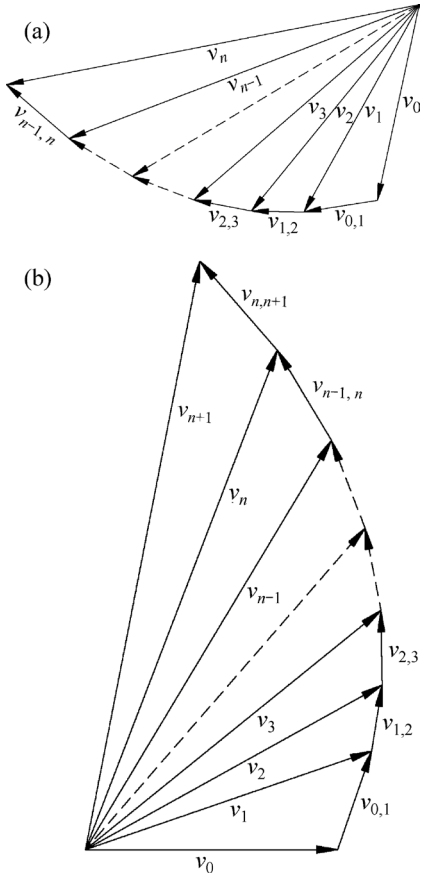

Fig. 3 Velocity fields of a pressurized tunnel: (a) Active failure mechanism; (b) Passive failure mechanism

Similarly, according to Fig. 3(b), the velocities of passive failure mechanism can be written as

$$v_1=\frac{\sin(\pi/2+\varphi_t)}{\sin(\pi/2-\alpha_1-\varphi_t)}v_0 \tag{28}$$

$$v_{0,1}=\frac{\sin(\alpha_1+\varphi_t)}{\sin(\pi/2-\alpha_1-\varphi_t)}v_0 \tag{29}$$

$$v_i=\frac{\sin(\pi/2+\varphi_t)}{\sin(\pi/2-\alpha_i-\varphi_t)}v_{i-1}\ (i=2,\cdots,n) \tag{30}$$

$$v_{i-1,i}=\frac{\sin\alpha_i}{\sin(\pi/2-\alpha_i-\varphi_t)}v_{i-1}\ (i=2,\cdots,n) \tag{31}$$

$$v_{n+1}=\sin(\pi/2+\varphi_t)\cdot v_n/\sin\sum_{i=1}^{n}\alpha_i \tag{32}$$

$$v_{n,n+1}=\sin\left(\pi/2-\sum_{i=1}^{n}\alpha_i-\varphi_t\right)\cdot v_n/\sin\sum_{i=1}^{n}\alpha_i \tag{33}$$

4 Calculation of retaining pressure for a pressurized tunnel face

This work aims to obtain the range of safe retaining pressures for the pressurized tunnel based on limit

analysis and reliability theory. The failure mechanism of pressurized tunnel face is simplified to a 2D plane strain problem. The geotechnical material is considered as ideal plastic material, and obeys the associated flow rule, and energy dissipation only exists along the velocity discontinuity.

For a pressurized tunnel, the power of external forces consists of the power of soil gravity P_γ, the work rate of pore water pressure P_u, and the power of retaining pressure P_T. And the total energy dissipation P_V is the sum of energy dissipation on every velocity discontinuities.

4.1 Upper bound solution of active failure mechanism

For the convenience of calculation, the disconnections OA, OB_1, B_1B_2, ⋯, $B_{n-1}B_n$, B_nB, AB_1, ⋯, AB_n in Fig. 2(a) are projected on the surface of earth, and their projection areas are S_1, S_2, S_{11}, ⋯, S_{1n-1}, S_{1n}, S_{21}, ⋯, S_{2n}, respectively. Then, for the active failure mechanism, the power of external forces and energy dissipation can be written as follows:

$$\begin{aligned}P_\gamma = {} & \gamma\cdot S_{\Delta OAB_1}\cdot v_0\cdot\cos\left(\pi/2-\sum_{i=1}^{n}\alpha_i-\beta-\varphi_t\right)+\\ & \gamma\cdot S_{\Delta AB_1B_2}\cdot v_1\cdot\cos\left(\pi/2-\sum_{i=1}^{n}\alpha_i+\varphi_t\right)+\\ & \gamma\cdot S_{\Delta AB_2B_3}\cdot v_2\cdot\cos\left(\pi/2-\sum_{i=2}^{n}\alpha_i+\varphi_t\right)+\cdots+\\ & \gamma\cdot S_{\Delta AB_{n-1}B_n}\cdot v_{n-1}\cdot\cos\left(\pi/2-\sum_{i=n-1}^{n}\alpha_i+\varphi_t\right)+\\ & \gamma\cdot S_{\Delta AB_nB}\cdot v_n\cdot\cos(\pi/2-\alpha_n+\varphi_t)\end{aligned} \tag{34}$$

$$P_T=-\sigma_T\cdot D\cdot v_n\cdot\sin(\pi/2-\alpha_n+\varphi_t) \tag{35}$$

$$\begin{aligned}P_u = {} & \gamma\cdot r_u\cdot\sin\varphi_t\cdot(S_1\cdot v_0+S_2\cdot v_0+S_{11}\cdot v_1+\cdots+S_{1n}\cdot v_n+\\ & S_{21}\cdot v_{0,1}+\cdots+S_{2n}\cdot v_{n-1,n})\end{aligned} \tag{36}$$

$$\begin{aligned}P_V = {} & c_t\cdot\cos\varphi_t\cdot(OA\cdot v_0+OB_1\cdot v_0+B_1B_2\cdot v_1+\cdots+\\ & B_{n-1}B_n\cdot v_{n-1}+B_nB\cdot v_n+AB_1\cdot v_{0,1}+\cdots+\\ & AB_n\cdot v_{n-1,n})\end{aligned} \tag{37}$$

According to the virtual power principle, the collapse pressure σ_c on the face can be determined through equating the external work rate to the internal energy dissipation. The expression can be written as

$$\sigma_c=\sigma_T=\frac{P_\gamma+P_u-P_V}{D\cdot v_n\cdot\sin(\pi/2-\alpha_n+\varphi_t)} \tag{38}$$

$$\text{s.t.}\begin{cases}0<\alpha_i<\pi/2-\varphi_t\ (i=1,2,3,\cdots n-1)\\ \pi/2-\varphi_t<\beta<\pi\\ 0<\varphi_t<\pi/4\end{cases} \tag{39}$$

According to Eq. (38), σ_c is a function of α_1, α_2, α_3, ⋯, α_n, β and φ_t, namely $\sigma_c=f(\alpha_1, \alpha_2, \alpha_3, \cdots, \alpha_n, \beta, \varphi_t)$. The maximization of σ_c given by Eq. (38) is the critical collapse pressure. Under the constraints of Eq. (39), the maximization of the objective function $\sigma_c=f(\alpha_1, \alpha_2, \alpha_3, \cdots, \alpha_n, \beta, \varphi_t)$ can be achieved with Matlab software. Then, the maximum value corresponds to the lower-bound to ensure the safety of a pressurized tunnel. The point O is below the earth according to the optimization results.

4.2 Upper bound solution of passive failure mechanism

For the convenience of calculation, the disconnections B_nO_2, BB_1, B_1B_2, ⋯, $B_{n-1}B_n$, AB_1, ⋯, AB_n in Fig.2(b) are projected on the earth surface, and their projection areas are S_1, S_{11}, S_{12}, ⋯, S_{1n}, S_{21}, ⋯, S_{2n}, respectively. In this case, the power of external forces and energy dissipation can be obtained:

$$\begin{aligned}P_\gamma = {} & \gamma\cdot S_{\Delta ABB_1}\cdot v_1\cdot\cos(\pi/2-\alpha_1-\varphi_t)+\gamma\cdot S_{\Delta AB_1B_2}\cdot\\ & v_2\cdot\cos\left(\pi/2-\sum_{i=1}^{2}\alpha_i-\varphi_t\right)+\cdots+\gamma\cdot S_{\Delta AB_{n-1}B_n}\cdot v_n\cdot\\ & \cos\left(\pi/2-\sum_{i=1}^{n}\alpha_i-\varphi_t\right)+\gamma\cdot S_{\Delta AO_1O_2B_n}\cdot v_{n+1}\cos\varphi_t\end{aligned} \tag{40}$$

$$P_T=-\sigma_T\cdot D\cdot v_0 \tag{41}$$

$$\begin{aligned}P_u = {} & \gamma\cdot r_u\cdot\sin\varphi_t\cdot(S_1\cdot v_{n+1}+S_{11}\cdot v_1+\cdots+S_{1n}\cdot v_n+\\ & S_{21}\cdot v_{1,2}+\cdots+S_{2n}\cdot v_{n,n+1})\end{aligned} \tag{42}$$

$$\begin{aligned}P_V = {} & c_t\cdot\cos\varphi_t\cdot(BB_1\cdot v_1+B_1B_2\cdot v_2+\cdots+B_{n-1}B_n\cdot v_n+\\ & B_nO_2\cdot v_{n+1}+AO_1\cdot v_{n+1}+AB_1\cdot v_{1,2}+\cdots+\\ & AB_n\cdot v_{n,n+1})\end{aligned} \tag{43}$$

Likewise, according to the virtual power principle, the retaining pressure σ_T on the face can be determined by equating the external work rate to the internal energy dissipation, namely the blowout pressure σ_b under the passive failure mechanism. The expression can be written as

$$\sigma_b=\sigma_T=(P_\gamma+P_u-P_V)/(D\cdot v_0) \tag{44}$$

$$\text{s.t.}\begin{cases}0<\alpha_i<\pi/2-\varphi_t\ (i=1,2,3,\cdots n)\\ 0<\varphi_t<\pi/4-\left|\sum_{i=1}^{n}\alpha_i\right|/2\end{cases} \tag{45}$$

According to Eq. (44), σ_b is a function of α_1, α_2, α_3, ⋯, α_n and φ_t, i.e., $\sigma_b=f(\alpha_1, \alpha_2, \alpha_3, \cdots, \alpha_n, \varphi_t)$. In order to get the critical blowout pressure, the minimum value of σ_b must be worked out. Under the constraints of Eq. (45), the minimization of the objective function $\sigma_b=f(\alpha_1, \alpha_2, \alpha_3, \cdots, \alpha_n, \varphi_t)$ is obtained using Matlab software. Then, the critical blowout pressure is the maximum support force to ensure the pressurized tunnel without

blowout happening.

4.3 Reliability model

For the objective existence of parameter randomness of soil and its influence on the stability of pressurized tunnel, it is more scientific and rational to solve the range of safe retaining pressure applying reliability theory after using limit analysis with nonlinear failure criterion.

σ_c is the lower-bound against the collapse and σ_b is the upper-bound value to prevent blow-out, so the retaining pressure σ_T that ensures the safety of a pressurized tunnel excavation surface must satisfy

$$g_1(X)=\sigma_T-\sigma_c>0 \tag{46}$$

$$g_2(X)=\sigma_b-\sigma_T>0 \tag{47}$$

For single failure mode, when pressurized tunnel collapses or blowouts, the reliability models are respectively

$$R_s=P\{g_1(X)>0\} \tag{48}$$

$$R_s=P\{g_2(X)>0\} \tag{49}$$

With respect to multiple failure modes, the reliability model of pressurized tunnel is expressed as follows:

$$R_s=P\{g_1(X)>0\cap g_2(X)>0\} \tag{50}$$

5 Numerical results and discussion

5.1 Number *n* of triangle rigid blocks

The number of the rigid blocks of failure mechanism directly influences the precision of the calculation results. In order to strike a balance between the accuracy of the critical pressure for a pressurized tunnel and computation time, the number of triangle rigid blocks is discussed here. Table 1 presents the values of collapse pressure σ_c and blowout pressure σ_b with different n corresponding to tunnel diameter D=10 m, buried depth C=10 m, soil bulk density γ=20 kN/m^3, nonlinear coefficient m=1.2, initial cohesion c_0=10 kPa and axial tensile stress σ_t=30 kPa. It is found from Table 1 that the precision of the earth pressure can be improved with the increase of the number n of triangle rigid blocks. When n=5, the improvement of the collapse pressure σ_c and blowout pressure σ_b is within 1%, satisfying the precision requirements. Therefore, the value of n is chosen to be 5 throughout the numerical computation.

Table 1 Influence of number n of triangle rigid blocks on earth pressure

n	σ_c		σ_b	
	Value/kPa	Improvement/%	Value/kPa	Improvement/%
1	75.8	—	898.8	—
2	86.4	14	806.5	10
3	92.1	7	776.8	4
4	95.7	4	762.3	2
5	96.3	1	753.8	1

5.2 Comparison validation

In order to verify the rationality of the failure mechanism and the correctness of the calculation method, the nonlinear failure criterion will degenerate into the linear MC failure criterion with the nonlinear coefficient being equal to 1. Then, the calculation results are compared with the numerical simulation results, as shown in Fig. 4, with relevant parameters corresponding to: diameter D=10 m, buried depth C=10 m, soil bulk density γ=20 kN/m^3, cohesive force c=10 kPa and internal friction angle φ=18°. It can be found in Fig. 4 that, in contrast with the displacement reprogram of the numerical simulation results, the failure mechanism of this work agrees well with the numerical simulation solution. It can also be obtained that the earth pressure is also coincident with simulation results and the difference is less than 8%. Then, the rationality of the failure

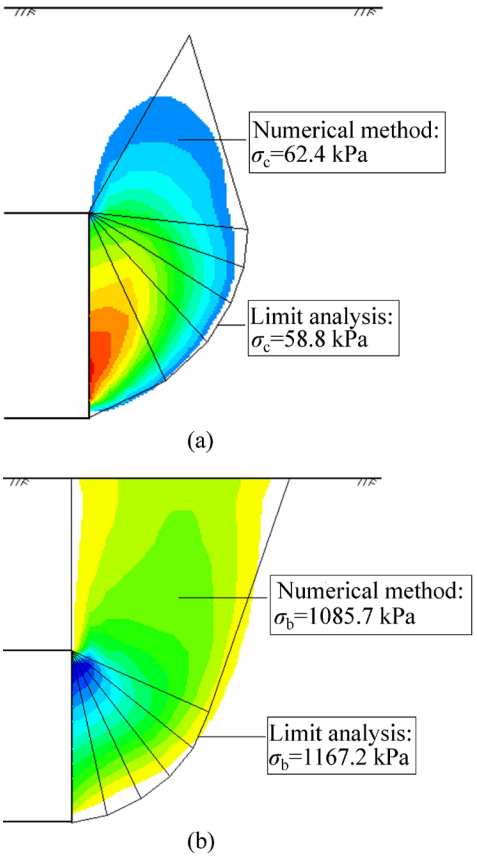

Fig. 4 Comparison of results between limit analysis and numerical simulations: (a) Active failure mechanism; (b) Passive failure mechanism

mechanism and the validity of the calculation method are verified with the consistency.

5.3 Sensitivity analysis

In the case of D=10 m and C=10 m, sensitivity analysis is conducted to discuss the impact of random variables on the reliability of pressurized tunnel. Since the results are the same, the sensitivity factors of random variables are solved only for the active failure mechanism, and the statistical properties are given in Table 2, in which σ_T is equal to σ_c. The sensitivity factors of random variables of a pressurized tunnel are illustrated in Fig. 5. It is obvious to see that the reliability is most sensitive to the nonlinear coefficient m and pore water pressure coefficient r_u, initial cohesive c_0 and soil bulk density γ rank the second, while the reliability is not very sensitive to retaining pressure σ_T and axial tensile stress σ_t. It is shown that the nonlinear coefficient and pore water pressure coefficient are the main factors which influence the reliability of pressurized tunnel.

Table 2 Statistical property of random variables (I)

Random variable	Mean	Standard deviation	Coefficient of variation	Type of distribution
M	1.2	0.18	0.15	Gaussian
c_0/kPa	10	1.5	0.15	Gaussian
σ_t/kPa	30	4.5	0.15	Gaussian
γ/(kN·m^{-3})	20	3	0.15	Gaussian
r_u	0.2	0.03	0.15	Gaussian
σ_T/kPa	113.4	17.0	0.15	Gaussian

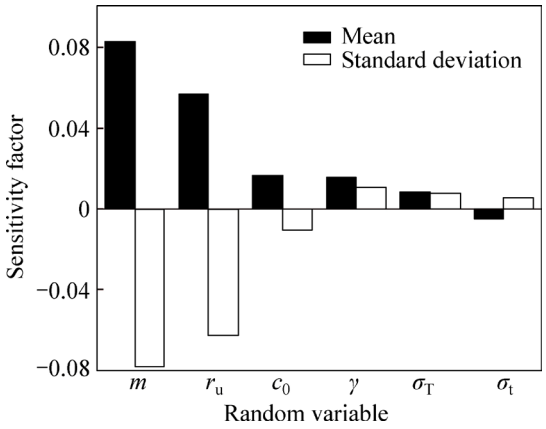

Fig. 5 Comparison on sensitivity factors of distribution parameters of random variables

5.4 Influence of coefficient of variation on reliability

The statistic characteristics of random variables are given in Table 3 when $\sigma_{T1}=\sigma_c$, $\sigma_{T2}=\sigma_b$, tunnel diameter D=10 m and cover depth C=10 m. The effect of variation coefficient on the reliability of pressurized tunnel is illustrated in Fig. 6. According to Fig. 6, both for active failure mechanism and passive failure mechanism, the

Table 3 Statistical property of random variables (II)

Random variable	Mean	Coefficient of variation	Type of distribution
m	1.2	0.15	Lognormal
r_u	0.2	0.15	Lognormal
c_0/kPa	10	0.15	Lognormal
σ_t/kPa	30	0.15	Lognormal
γ/(kN·m^{-3})	20	0.15	Lognormal
σ_{T1}/kPa	113.4	0.15	Gaussian
σ_{T2}/kPa	790.3	0.15	Gaussian

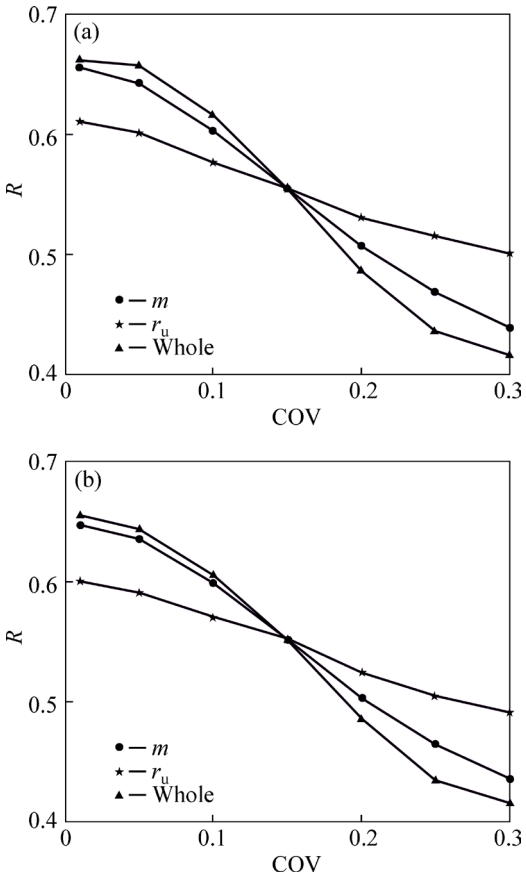

Fig. 6 Influence of variation coefficients on reliability: (a) Active failure mechanism; (b) Passive failure mechanism

reliability tends to decrease with the increase of variation coefficient of nonlinear coefficient m or pore water pressure coefficient r_u. The variation coefficient of nonlinear coefficient m has a more obvious effect on reliability. In addition, it is worth noticing that when the overall variation coefficients increase together, the reliability reduces significantly. It can be concluded that the variation coefficient which represents the parameter randomness of soil has a great impact on the reliability of pressurized tunnel, especially the variation coefficients of nonlinear coefficient m and pore water pressure coefficient r_u. Therefore, it is suggested that the parameter randomness of soil should be considered in the design of retaining structures, and the variability level of

geotechnical parameters should also be improved simultaneously.

5.5 Range of safe retaining pressure

In the view of the main influence factors, the range of safe retaining pressure for a pressurized tunnel is presented by considering the parameter randomness of soil or neglecting it with tunnel diameter D=10 m and cover depth C=10 m.

5.5.1 Range of safe retaining pressure without considering parameter randomness of soil

Without considering the parameter randomness of soil, the influences of nonlinear coefficient m and pore water pressure coefficient r_u on earth pressure are illustrated in Fig. 7, with other parameters corresponding to soil bulk density γ=20 kN/m^3, initial cohesion c_0=10 kPa and axial tensile stress σ_t=30 kPa. According to Fig. 7, the collapse pressure σ_c shows a trend of increase with the increasing values of nonlinear coefficient m and pore water pressure coefficient r_u under active failure mechanism. However, the blowout pressure σ_b is positive to pore water pressure coefficient r_u but decreases with the increase of nonlinear coefficient m under passive failure mechanism. Table 4 gives the range of safe retaining pressure according to the data obtained in Fig. 7.

5.5.2 Range of safe retaining pressure in consideration with parameter randomness of soil

Considering the parameter randomness of soil, it is assumed that the statistic characteristics of random variables are shown in Table 5. The failure probabilities of a pressurized tunnel under single failure mode and

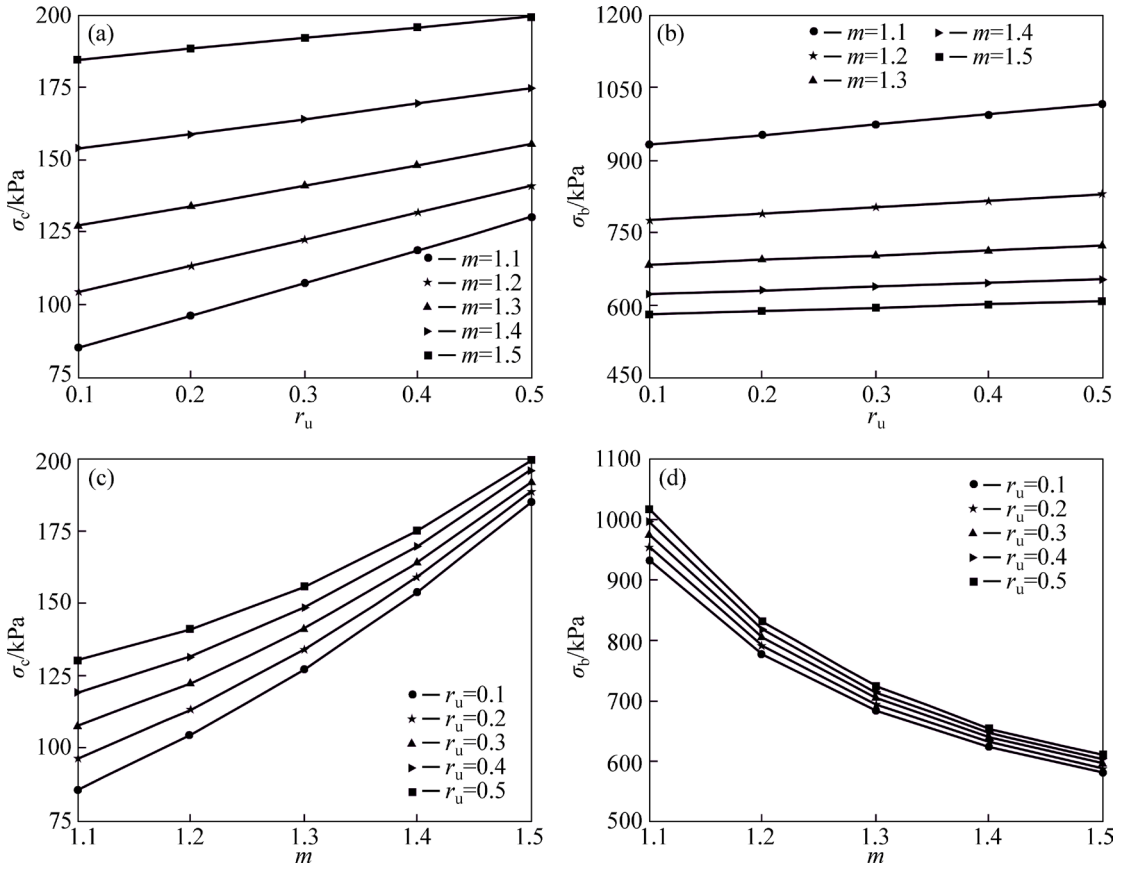

Fig. 7 Influences of nonlinear coefficient and pore water pressure coefficient on earth pressure: (a) r_u−m−σ_c; (b) r_u−m−σ_b; (c) m−r_u−σ_c; (d) m− r_u−σ_b

Table 4 Range of safe retaining pressure without regard to parameter randomness of soil

m	Range of safe retaining pressure/kPa				
	r_u=0.1	r_u=0.2	r_u=0.3	r_u=0.4	r_u=0.5
1.1	85.3−931.9	96.4−953.3	107.5−974.6	118.9−995.8	130.4−1016.9
1.2	104.5−776.4	113.4−790.3	122.4−804.1	131.6−817.9	141.0−831.4
1.3	127.2−684.0	134.0−694.1	141.0−704.0	148.2−713.9	155.5−723.6
1.4	153.9−623.3	158.9−631.0	164.1−638.6	169.4−646.2	174.8−653.6
1.5	185.0−580.5	188.5−586.7	192.1−592.8	195.8−598.8	199.6−604.8

Table 5 Statistical properties of random variables (III)

Random variable	Mean	COV	Type of distribution
m	1.1−1.5	0.15	Lognormal
r_u	0.1−0.5	0.15	Lognormal
c_0/kPa	10	0.15	Lognormal
σ_t/kPa	30	0.15	Lognormal
γ/(kN·m^{-3})	20	0.15	Lognormal
σ_T/kPa	—	0.15	Gaussian

multiple failure modes are illustrated in Fig. 8 and Fig. 9 respectively. In Fig. 8, with the mean of retaining pressure increasing, the failure probability of a pressurized tunnel in active failure mechanism shows a trend of decrease, while a trend of increase in passive failure mechanism.

In Fig. 9, with the increase of the mean of retaining pressure, the failure probability of a pressurized tunnel decreases at first and then increases. Thus, as for multiple failure modes, when the mean of retaining pressure is less than the value of the lowest point on the curve, the probability for collapse is larger; when the mean of retaining pressure is greater than the value of the lowest point on the curve, the probability for blowout is greater. The value of the lowest point on the curve is the best mean of retaining pressure for pressurized tunnel face.

For the failure probability of a pressurized tunnel against multiple failure modes, as shown in Fig. 9, the range of safe retaining pressure for a pressurized tunnel can be obtained by introducing the allowable failure probability [P_f]. As given in Table 6, different ranges of safe retaining pressure can be obtained when nonlinear coefficient m increases linearly from 1.1 to 1.5 and pore water pressure coefficient r_u increases linearly from 0.1 to 0.5, allowable failure probability [P_f] decreasing nonlinearly from 0.1 to 0.00001. Different allowable failure probabilities also correspond to different ranges of safe retaining pressure, so the optimal range of safe retaining pressure for a pressurized tunnel can be obtained by seeking the minimum allowable failure probability. As shown in Fig. 10, when the allowable failure probabilities [P_f] are equal to 0.1, 0.01 and 0.001, the ranges of safe retaining pressure are 166−588 kPa, 226−471 kPa, and 291−399 kPa, respectively, for the case of the nonlinear coefficient m=1.2, pore water pressure coefficient r_u=0.2, but it cannot be satisfied that the allowable failure probability is 0.0001. Then, the optimal range of safe retaining pressure for a pressurized tunnel can be obtained as 324−373 kPa corresponding to the minimum allowable failure probability is $[P_f]_{min}$= 0.0005.

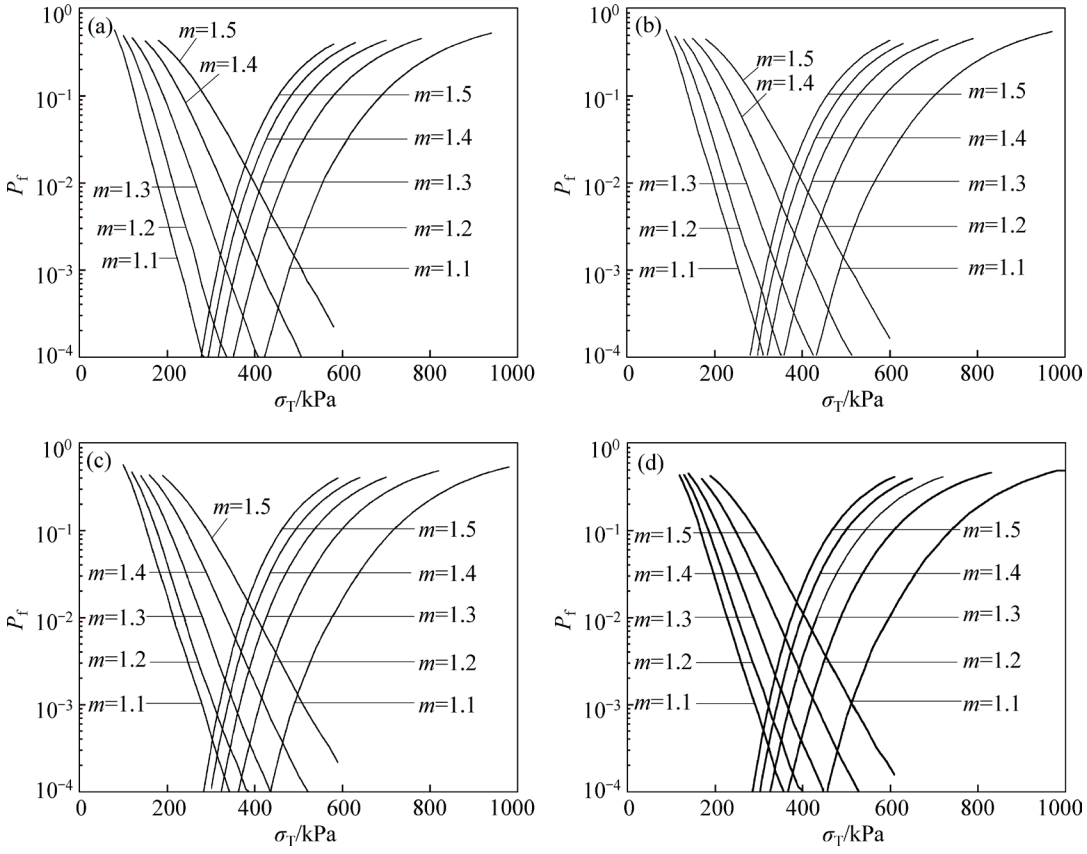

Fig. 8 Influence of mean of retaining pressure on failure probability with regard to a single failure mode: (a) r_u=0.1; (b) r_u=0.2; (c) r_u=0.3; (d) r_u=0.4

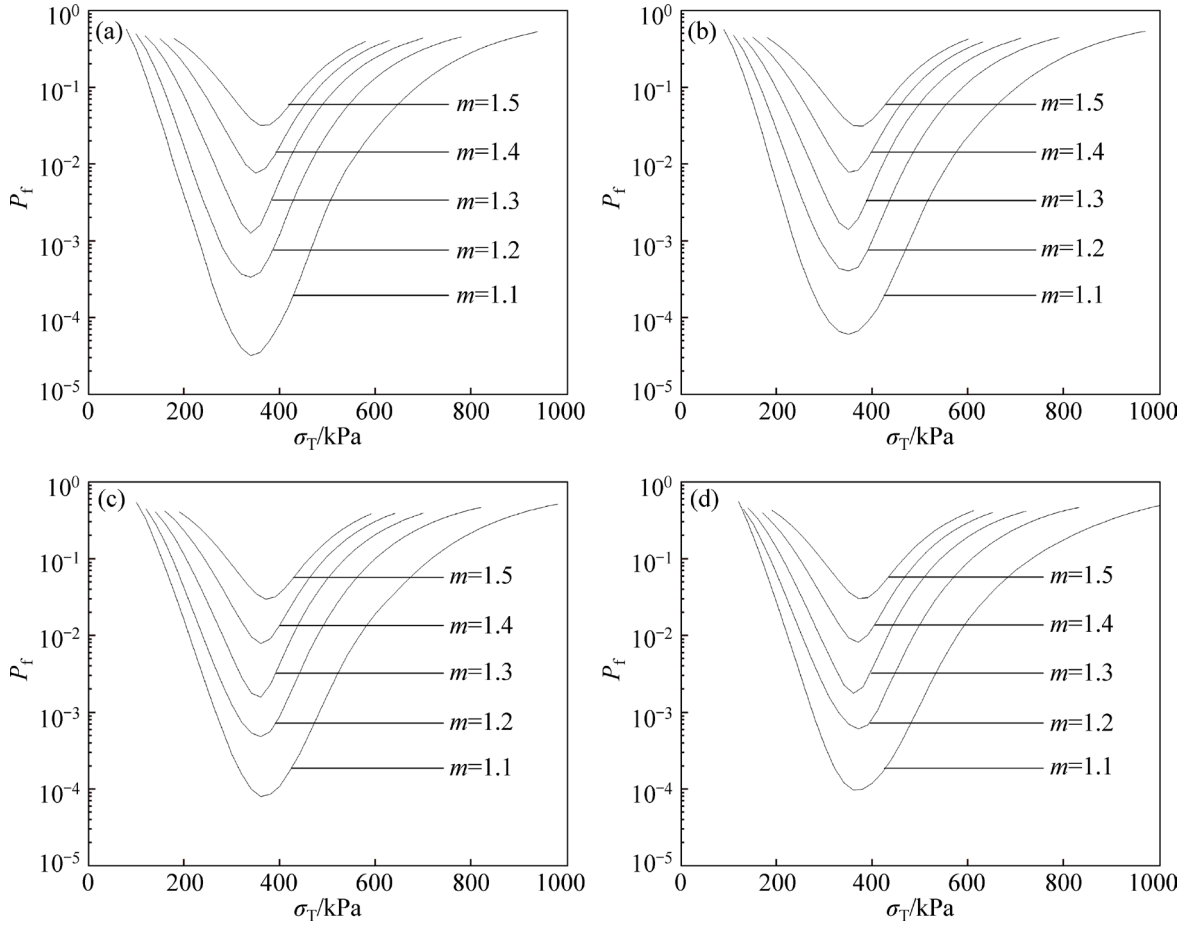

Fig. 9 Influence of mean of retaining pressure on failure probability against multiple failure modes: (a) r_u=0.1; (b) r_u=0.2; (c) r_u=0.3; (d) r_u=0.4

Table 6 Range of safe retaining pressures with regard to parameter randomness of soil

m	r_u	Range of safe retaining pressures/kPa				$[P_f]_{min}$	Optimal range/kPa
		$[P_f]$=0.1	$[P_f]$=0.01	$[P_f]$=0.001	$[P_f]$=0.0001		
1.1	0.1	131−686	180−546	234−471	288−406	0.0001	288−406
	0.2	142−700	194−557	246−475	310−395	0.0001	310−395
	0.3	156−714	208−566	260−481	334−382	0.0001	334−382
	0.4	170−728	222−576	275−489	358−369	0.0001	358−369
	0.5	184−742	236−587	290−497	—	0.0002	345−413
1.2	0.1	157−578	214−464	274−394	—	0.0004	314−362
	0.2	166−588	226−471	291−399	—	0.0005	324−373
	0.3	176−597	239−478	309−403	—	0.0006	334−382
	0.4	186−606	252−485	328−406	—	0.0007	350−387
	0.5	197−615	266−491	351−408	—	0.0008	367−394
1.3	0.1	192−521	265−416	—	—	0.002	314−368
	0.2	199−528	272−421	—	—	0.002	324−371
	0.3	205−535	281−426	—	—	0.002	335−373
	0.4	212−541	290−431	—	—	0.002	348−375
	0.5	220−548	299−436	—	—	0.003	341−395

to be continued

Continued

m	r_u	Range of safe retaining pressure/kPa				$[P_f]_{min}$	Optimal range/kPa
		$[P_f]$=0.1	$[P_f]$=0.01	$[P_f]$=0.001	$[P_f]$=0.0001		
1.4	0.1	234−482	329−378	—	—	0.008	343−364
	0.2	239−487	334−381	—	—	0.008	350−367
	0.3	243−493	340−385	—	—	0.008	360−369
	0.4	248−498	345−388	—	—	0.009	353−381
	0.5	252−503	352−391	—	—	0.009	359−383
1.5	0.1	286−451	—	—	—	0.04	338−398
	0.2	289−455	—	—	—	0.04	340−402
	0.3	291−460	—	—	—	0.04	342−406
	0.4	294−464	—	—	—	0.04	345−410
	0.5	296−468	—	—	—	0.04	347−414

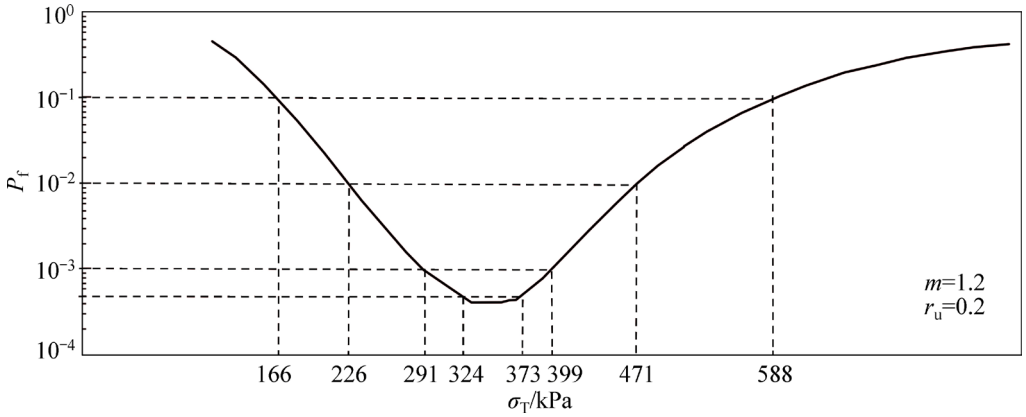

Fig. 10 Range of safe retaining pressures of pressurized tunnel faces with different allowable failure probabilities

As a result, the importance of parameter randomness of soil is proved by the results of Table 6. If the parameter randomness of soil is not taken into account, collapse or blowout damage may take place even if the retaining pressure of a pressurized tunnel satisfies safe requirement. In short, it will be more scientific and rational to utilize the reliability theory for the design of a pressurized tunnel. The results in Table 6 can provide important reference for design and construction of pressurized tunnels in the future.

6 Conclusions

1) In order to meet the accuracy of results and the time-costing requirement, the number of triangle rigid blocks is discussed, and the result can satisfy the relevant requirements simultaneously with n=5.

2) The present solutions are compared with numerical simulation results when the nonlinear failure criterion degenerates into the linear MC failure criterion, with nonlinear coefficient m=1.0. The rationality of the failure mechanism and the correctness of the calculation method are verified by the consistency of displacement reprogram and agreement of earth pressure.

3) In the sensitivity analysis of random variables, nonlinear coefficient and pore water pressure coefficient have a significant effect on reliability, whereas initial cohesion and soil bulk density have a less impact. The retaining pressure and axial tensile stress almost have no effect on the reliability. Thus, nonlinear coefficient and pore water pressure coefficient are the principal factors which affect the reliability of structure system for a pressurized tunnel.

4) According to the maximum entropy principle, the soil parameters are assumed to obey the most common and important normal distribution and lognormal distribution, respectively. The variation coefficient which represents the parameter randomness of soil has a large impact on the reliability of a pressurized tunnel. The research of the statistical distribution and the analysis of variability level should be further improved.

5) Ranges of safe retaining pressure for a pressurized tunnel in multiple failure modes are solved by referring to the parameter randomness of soils and introducing allowable failure probability. If the parameter randomness of soils is not considered, collapse or blowout damage might take place even if the retaining

pressure is between the collapse pressure and the blowout pressure.

References

[1] LECA E, DORMIEUX L. Upper and lower bound solutions for the face stability of shallow circular tunnels in frictional material [J]. Géotechnique, 1990, 40(4): 581−606.

[2] HUANG F, QIN C B, LI S C. Determination of minimum cover depth for shallow tunnel subjected to water pressure [J]. Journal of Central South University, 2013, 20(8): 2307−2313.

[3] SUBRIN D, WONG H. Tunnel face stability in frictional material: A new 3D failure mechanism [J]. Computes Rendus Mecanique, 2002, 330(7): 513−519.

[4] KLAR A, OSMAN A S, BOLTON M. 2D and 3D upper bound solutions for tunnel excavation using elastic flow fields [J]. International Journal for Numerical and Analytical Methods in Geomechanics, 2007, 31(12): 1367−1374.

[5] MOLLON G, DIAS D, SOUBRA A H. Range of the safe retaining pressures of a pressurized tunnel face by a probabilistic approach [J]. Journal of Geotechnical and Geoenvironmental Engineering, 2013, 139(11): 1954−1967.

[6] HOEK E, BROWN E T. Practical estimate the rock mass strength [J]. International Journal of Rock Mechanics and Mining Sciences, 1997, 34(8): 1165−1186.

[7] SHIN J H. Analytical and combined numerical methods evaluating pore water pressure on tunnels [J]. Géotechnique, 2010, 60(2): 141−145.

[8] SENENT S, MOLLON G, JIMENEZ R. Tunnel face stability in heavily fractured rock masses that follow the Hoek-Brown failure criterion [J]. International Journal of Rock Mechanics and Mining Sciences, 2013, 60(1): 440−451.

[9] SAADA Z, MAGHOUS S, GARNIER D. Pseudo-static analysis of tunnel face stability using the generalized Hoek-Brown strength criterion [J]. International Journal for Numerical and Analytical Methods in Geomechanics, 2013, 37(18): 3194−3212.

[10] SOUBRA A H. Three-dimensional face stability analysis of shallow circular tunnels [C]// International Conference on Geotechnical and Geological Engineering. Melbourne, Australia, 2000: 19−24.

[11] YANG Xiao-li, QIN Chang-bing. Limit analysis of supporting pressure in tunnels with regard to surface settlement [J]. Journal of Central South University, 2015, 22(1): 303−309.

[12] HUANG K, LIU B C, PENG J G, HUANG F. Limit analysis of supporting pressure for failure surface of deep-buried tunnel with nonlinear failure criterion [J]. Advanced Materials Research, 2012, 443−444: 962−969.

[13] CHEN X W, DAI W. Maximum entropy principle for uncertain variables [J]. International Journal of Fuzzy Systems, 2011, 13(3): 232−236.

[14] YANG X L, PAN Q J. Three dimensional seismic and static stability of rock slopes [J]. Geomechanics and Engineering, 2015, 8(1): 97−111.

[15] YANG X L, YAN R M. Collapse mechanism for deep tunnel subjected to seepage force in layered soils [J]. Geomechanics and Engineering, 2015, 8(5): 741−756.

[16] XU Zhi-jun, ZHENG Jun-jie, BIAN Xiao-ya, LIU Yong. A modified method to calculate reliability index using maximum entropy principle [J]. Journal of Central South University, 2013, 20(4): 1058−1063.

[17] MOLLON G, DIAS D, SOUBRA A H. Probabilistic analyses of tunneling-induced ground movements [J]. Acta Geotechnica, 2013, 8(2): 181−199.

(Edited by YANG Bing)